Binding Free Energy Calculations of Adenosine Deaminase Inhibitor and the Effect of Methyl Substitution in Inhibitors

Takahiro Kosugi, Isao Nakanishi,* and Kazuo Kitaura

Graduate School of Pharmaceutical Sciences, Kyoto University, Sakyo-ku, Kyoto 606-8501, Japan

Received July 14, 2008

The binding affinity of an inhibitor is often improved ten times or more by introducing a simple substituent, such as a methyl group or a chlorine atom. We have investigated this phenomenon in the case of adenosine deaminase (ADA) inhibitors using molecular dynamics (MD) simulations and binding free energy calculations, by the linear interaction energy (LIE) method. For MD simulations, the coordination bond parameters and partial charges of atoms around the zinc ion in ADA have been determined by referring to *ab initio* MO calculations. The calculated binding free energies for seven inhibitors agreed well with the experimental ones, with a maximum error of 1.2 kcal/mol. The effect of methyl substitution in inhibitor molecules was examined on the basis of MD trajectories. It is suggested that the increase in binding affinity is caused by both van der Waals stabilizations by amino acid residues in contact with the introduced methyl group and through favored overall interactions with surrounding residues in the binding pocket.

INTRODUCTION

In drug design, computational prediction of protein−ligand binding affinity helps lead generation and optimization by displaying important interaction sites for binding, especially in the case of very simple chemical modifications such as the introduction of a methyl group or a chlorine atom that dramatically improves the binding affinity. Although this phenomenon is occasionally observed,[1−3] the real factors affecting it or mechanisms through which it operates have not been determined and discussed in detail. Medicinal chemists introduce such substitutents based on experience, without conviction, and occasionally succeed in improving the binding affinity. In a structure-based approach, if a gap is found at the protein−ligand interface, one is prompted to introduce bulky substituents to fill the gap, expecting that closer contact might strengthen the protein−ligand binding. Computer simulations of such systems might provide more reliable prediction and explain why a substituent increases or decreases binding affinity. In this study, the binding free energies of a series of adenosine deaminase inhibitors were calculated, and the structure−activity relationship was investigated.

ADA is a metalloenzyme containing a zinc ion at the active site. It is an essential enzyme for purine metabolism and catalyzes the irreversible hydrolysis of adenosine and 2′-deoxyadenosine to inosine and 2′-deoxyinosine, respectively. ADA is known to be ubiquitous in almost all human tissues, and ADA abnormalities have been reported in a wide variety of diseases.[4−8] Recently, it has been revealed that ADA is involved in the regulation of the immune system[9−12] and inflammation.[13] ADA inhibitors, therefore, have potential as anti-inflammatory drugs or immunosuppressants. The toxicity and poor pharmacokinetics of known potent ADA inhibitors, such as pentostatin and (+)-EHNA, are due to their nucleoside molecular frameworks. Terasaka et al. discovered non-nucleoside ADA inhibitors with a imidazolecarboxamide nucleus based on structure-based drug design and computational methods.[14−17] They reported that the flexibility of the ADA active site made inhibitor design difficult. Therefore, it is desirable to take protein dynamics into consideration when predicting the binding affinities of ADA inhibitors.

We employed the linear interaction energy (LIE) method for calculating binding free energies between the protein and ligands (ΔG_{bind}). In the LIE method, MD simulations of both bound (in protein) and unbound (in water) states of a ligand are performed, and the simulation averages of the interaction energies between the ligand and its environment are used in the following equation[18]

$$\Delta G_{bind} = \alpha\langle \Delta V_{p-w}^{vdW} \rangle + \beta \langle \Delta V_{p-w}^{ele} \rangle \quad (1)$$

Here $\langle \Delta V_{p-w}^{vdW} \rangle$ and $\langle \Delta V_{p-w}^{ele} \rangle$ are the differences in the average van der Waals and electrostatic interaction energies, respectively, between bound and unbound states. The electrostatic interaction term usually has the coefficient β of 0.5, derived from linear response theory. The coefficient α for the van der Waals interaction term is an adjustable parameter for reproducing experimental binding free energies. The LIE method has been applied to a variety of proteins, such as HIV protease,[19−21] endothiapepsin,[18] glucose binding protein,[22] dihydrofolate reductase,[23] avidine,[24] and so on.[25−27] The calculated binding free energies were shown to be in good agreement with experimental values for these proteins. However, few applications to metalloproteins have been reported,[28−30] probably due to the lack of a common force field for the coordination bond of the metal ion.

The partial charge and coordination bond parameters of zinc ions in proteins have been examined by several researchers. Merz et al. studied force fields for zinc ions in human carbonic anhydrase II[31−33] (CAII) and zinc-β-lacta-

* Corresponding author phone: +81-6-6721-2332; fax: +81-6-6730-1394; e-mail: isayan@phar.kindai.ac.jp. Present address: Department of Pharmaceutical Sciences, Kinki University, 3-4-1 Kowakae, Higashi-Osaka 577-8502, Japan.

10.1021/ci8002667 CCC: $40.75
Published on Web 02/25/2009

mase.[34−36] They adopted a bonded approach that considers explicit bonds between zinc ions and coordinated atoms and succeeded in reproducing the experimental coordination geometry. Their approach, however, is computationally too expensive to use for generating parameters for each metalloprotein. Furthermore, their parameters may be insufficient to describe the flexibility of coordination bonds.[37,38] The alternative nonbonded models of coordination bonds include only modified nonbonded interactions,van der Waals and electrostatic terms.[37,38] These models are sensitive to the chosen electrostatic model and often suffer from an inability to retain the coordination number.[34,39]

We introduced a novel coordination bond model in which the bond is described by a covalent bond and nonbonded terms. The covalent bond parameters and atomic partial charges of atoms coordinated to zinc ions of adenosine deaminase (ADA) were generated referring to the *ab initio* potential energy surface of a model system. Our model does not use angle and torsion parameters and has proper flexibility of the coordination bonds.

This paper is organized as follows: The section on Computational Methods describes detailed procedures for the determination of coordination bond parameters and for MD simulations for the calculations of binding free energies; the Results and Discussion section first presents the structures and interaction energies of ADA-inhibitor complexes obtained from MD simulations with the new coordination bond parameters and then compares the binding free energies calculated by the LIE method with experimental values. Finally, the inhibitor recognition mechanism of ADA and the effect of methyl substitution in inhibitors are discussed on the basis of the analysis of MD trajectories.

COMPUTATIONAL METHODS

Partial Charges of Coordination Bond Atoms. We used electrostatic potential derived charges (ESP).[40] Figure 1a shows a model for the calculations of atomic partial charges, which is derived from the crystal structure of ADA-deazaadenosine complex (PDB: 1ADD).[41] The model system consists of a zinc ion, a water molecule, and coordinated residues—three histidine (His15, His17, His214) and one aspartic acid (Asp295). In addition, His238, which does not directly coordinate with the zinc ion, is included to determine the hydrogen atom positions of the water molecule. Both N- and C-terminus of the extracted amino acid residues were capped with acetyl and methylamine groups, respectively. Gly16 is regarded as the C-terminal cap of His15 and the N-terminal cap of His17. Missing hydrogen atoms were added using the LEaP module of AMBER8,[42] and their positions were optimized by the AM1 semiempirical MO method, keeping the coordinates of non-hydrogen atoms in the experimental positions. After the geometry optimization, His238 was removed from the model system.

The *ab initio* MO calculations were performed on this reduced model system at the HF level with the 6−31G* and LanL2DZ (for zinc ions) basis set using Gaussian03,[43] and ESP derived charges were calculated. For zinc ions, an ESP derived charge is used. We determined the atomic charges of each residue by the Lagrange multiplier method, to keep main chain and Cβ atomic charges close to the corresponding AMBER ff99 charges, since ESP derived charges of atoms

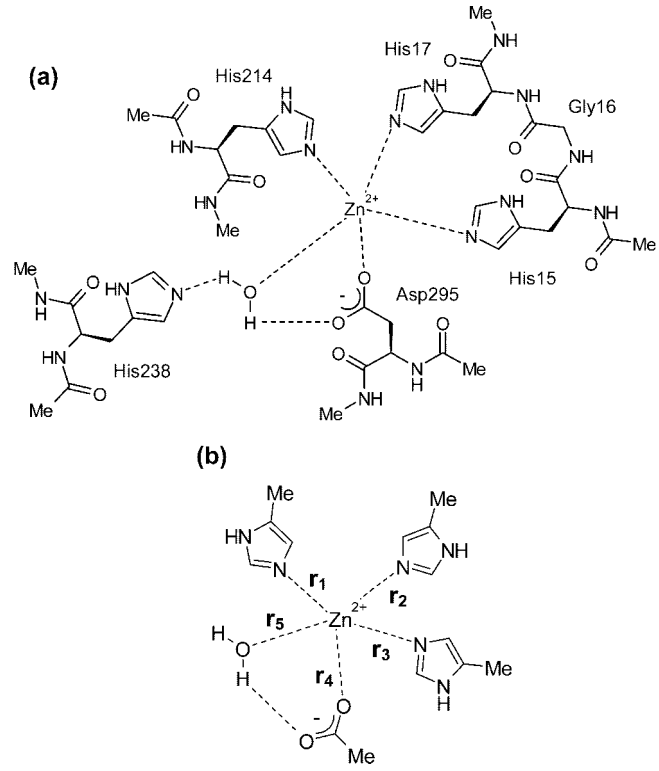

Figure 1. Model systems used to determine the ESP charge (a) and for coordination bond parameter determination (b). The His238 in model (a) was placed for the optimization of hydrogen atom positions and removed for ESP charge calculation.

buried by adjacent atoms tend to be poorly determined.[44] We assumed that charge transfers from residues to zinc ions would occur mostly from coordinated side chain atoms, and their charges should be close to ESP charges. Under this assumption, atomic partial charges were determined by minimizing the function μ for each capped residue

$$\mu = \{(q_1 - q_1^{\mathrm{ff99}})^2 + \cdots + (q_m - q_m^{\mathrm{ff99}})^2\} + \{(q_{m+1} - q_{m+1}^{\mathrm{ESP}})^2 + \cdots + (q_n - q_n^{\mathrm{ESP}})^2\} + \lambda\left\{\sum_{i=1}^{n} q_i - \sum_{i=1}^{n} q_i^{ESP}\right\}$$

where superscripts ff99 and ESP of q indicate AMBER ff99 and ESP charges, respectively. n is the total number of atoms in the residue, and m is the number of main chain atoms plus one (Cβ). q_i is the charge of the i-th atom to be determined. λ is a Lagrange multiplier, and the sum of fitted charges was restrained to reproduce that of the ESP derived charges.

Coordination Bond Parameters. We describe a coordination bond potential with a covalent term and nonbonded terms

$$U(r) = K_r(r - r_{\mathrm{eq}})^2 + \text{nonbonded terms} \qquad (2)$$

Here r is the distance between the zinc ion and the coordinate atom, and r_{eq} is the equilibrium distance, which is taken from the experimental geometry of ADA (PDB: 1ADD). The force constant K_r is determined by referring to the *ab initio* potential of a model system. A smaller model system than that used for ESP calculations was employed to save computation time, where histidine and aspartic acid residues were replaced by methylimidazole and charged acetic acid,

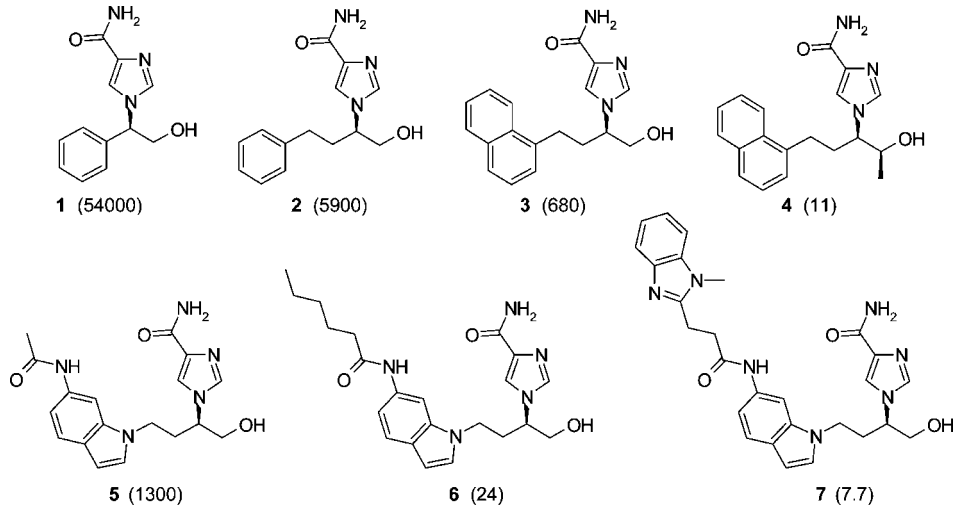

Figure 2. Chemical structures of ADA inhibitors used for binding free energy calculations. Experimental K_i values (nM)[14−17] are shown in parentheses. K_i values of inhibitor **1**, **2**, and **3** are measured with their racemates.

respectively (Figure 1b). Such truncated systems are often used for parameter determination.[37−39]

The model system was energy minimized at the HF level of theory with the 6−31G**, 6−31+G** (anionic oxygen), and LanL2DZ (zinc ion) basis sets. The *ab initio* potential energy curve was calculated along a vector **r** connecting a zinc ion and a coordinate atom (Figure 1b) for each coordination group, where the internal geometrical parameters of the coordinated group were fixed at the values of the minimum geometry. From the *ab initio* potential energies, the nonbonded contribution calculated with force field parameters (the second term of eq 2) was subtracted to obtain the potential curve corresponding to the first term of eq 2. Then, the parameter K_r was determined by fitting the covalent bond function to the nonbonded energy subtracted from the *ab initio* potential curve.

Modeling of ADA-Inhibitor Complexes. We picked the seven ADA inhibitor complexes shown in Figure 2. These inhibitors have various molecular sizes and a wide activity range that are measured by the same researchers. The inhibition constants of these inhibitors range from μM to nM. The initial geometries of ADA-inhibitor **2, 3, 4,** and **7** complexes were taken from PDB 1NDW, 1NDY, 2E1W, and 1NDZ, respectively. The complex structures of inhibitors **1**, **5**, and **6** were not reported, and they were modeled based on the inhibitor most similar to them. For all complexes, missing hydrogen atoms were added by the LEaP module of AMBER8, and the directions of the hydrogen-atom-involving bonds were manually adjusted to make reasonable hydrogen bonds with surrounding atoms. Care must be taken in modeling because the positions of hydrogen atoms in the initial structure strongly influence the results of MD simulations.

Although the charge states of acidic amino acid residues in protein are also important, their prediction is difficult. We determined the charge states of acidic residues located at the inhibitor binding site based on the proposed reaction mechanism of ADA[41] and possible hydrogen bonds with the inhibitor molecule with a neutral charged state. A standard charge state was assumed for other acidic residues. Thus, Asp296 and Glu217 were set as neutral, while other Asp and Glu were deprotonated. His157, His210, and His241, located at the protein surface far from inhibitor molecule, were protonated. A hydrogen atom was attached to the Nδ atom of neutral histidine residues, except for His105, His197, and His278. All Arg and Lys residues were protonated. Thus, the entire complex had a net charge of −6.

MD Simulations. The AMBER ff99 parameters were assigned to the protein, except for the atoms involved in the coordination bond with the zinc ion. The parameters mentioned above were applied to the zinc ion and the coordinate atoms. RESP charges[45] and a general Amber force field[46] were assigned to the inhibitor molecules.

For bound state simulations, a protein-inhibitor complex was placed in a water box of 80 Å × 80 Å × 80 Å, and six sodium ions were put in the box to neutralize the system. In an unbound state, water molecules were generated in a box of 65 Å × 65 Å × 65 Å. TIP3P[47] was used as a water model for the both state simulations. All MD simulations were carried out at 300 K with the SHAKE procedure to constrain hydrogen atoms from moving. In an unbound state, a harmonic position restraint of 100 kcal/mol/Å^2 was applied on the chiral carbon atom at the β position of the hydroxyl group in inhibitor molecules. Nonbonded interactions were cutoff at 10 Å, and the particle mesh Ewald (PME) method[48] was used for long-range electrostatic interactions. MD simulations were performed with a constant-NPT ensemble, except for the heating stage, where the NVT ensemble was used. An equilibration step of 300 ps, including a 20 ps heating step, was followed by a production run of 500 ps, with a time step of 1.0 fs, and trajectories were collected every 0.1 ps. The total simulation time was 800 ps for each complex.

Average van der Waals and electrostatic interaction energies were obtained from all 5000 snapshots from MD simulations and used in binding free energy calculations (eq 1). Nonbonded interactions were cut off at 20 Å, and sodium ions were neglected in the calculation.

The AMBER8 software suite was used for MD simulations. The CARNAL, ANAL, and PTRAJ modules were used to analyze trajectories. All MD simulations were run on a GION server (Xeon 3.06 GHz), and MO calculations were performed on the FUJITSU PRIMEPOWER HPC2500 at the Academic Center for Computing and Media Studies, of Kyoto University.

Table 1. Generated Atomic Partial Charges of Zinc Ions and Coordinated Amino Acid Residue Atoms[a]

atom	Amber[b]	His15	His17	His214	atom	Amber[b]	Asp295
N	−0.4157	−0.4337	−0.4234	−0.4240	N	−0.5163	−0.4804
Cα	0.0188	0.0111	0.0111	0.0105	Cα	0.0381	0.0740
C	0.5973	0.5896	0.5896	0.5890	C	0.5366	0.5725
O	−0.5679	−0.5756	−0.5756	−0.5762	O	−0.5819	−0.5460
Cβ	−0.0462	−0.0539	−0.0539	−0.0545	Cβ	−0.0303	0.0056
Cγ	−0.0266	0.2775	0.2095	0.3317	Cγ	0.7994	0.7497
Cδ	0.1292	−0.2166	−0.0090	−0.1342	Oδ1	−0.8014	−0.7397
Nδ	−0.3811	−0.3762	−0.2410	−0.1699	Oδ2	−0.8014	−0.5507
Cε	0.2057	0.1337	−0.1078	−0.1288	total[c]	−1.0000	−0.4143
Nε	−0.5727	−0.4021	−0.3716	−0.3468	Zn	2.0000	1.0807
total[c]	0.0000	0.0261	0.0026	0.2004	O(water)	−0.8340	−0.8858

[a] Only heavy atoms are listed. All atomic partial charges including hydrogen atoms are given in the Supporting Information. [b] Default partial charges in Amber ff99 parameter set. [c] Total charges of a residue including hydrogen atoms.

Table 2. Coordination Bond Parameters for Zinc Ions and Coordinated Atoms

coordinated atom	equilibrium distance[a] (Å)	force constant (kcal/mol/Å^2)
His15 (Nε)	2.24	29.04
His17 (Nε)	2.03	17.73
His214 (Nε)	2.05	19.05
Asp295 (Oδ2)	2.27	34.14
WAT (O)	1.80	28.47

[a] Values were taken from the crystal structure (1ADD).

Table 3. Average Distances (Å) between the Zinc Ion and Coordinated Atoms[a]

	inhibitor			
	2	**3**	**4**	**7**
HIS15 (Nε)	2.2 (2.0)	2.2 (2.0)	2.2 (2.0)	2.2 (2.0)
HIS17 (Nε)	2.1 (1.9)	2.1 (2.0)	2.1 (2.0)	2.1 (2.0)
HIS214 (Nε)	2.2 (2.2)	2.2 (2.2)	2.2 (2.7)	2.2 (2.2)
ASP295 (Oδ1)	2.3 (2.6)	2.2 (2.3)	2.3 (2.2)	2.3 (2.3)
WAT (O)	1.9 (1.9)	1.9 (2.0)	1.9 (2.5)	1.9 (2.0)

[a] Distances observed in the crystal structure are given in parentheses.

RESULTS AND DISCUSSION

Coordination Bond Parameters. The partial charges of zinc ions and atoms of coordinated groups are listed in Table 1. The partial charge of a zinc ion is +1.08, which is within the range of previously reported values, from +0.69 to +1.2, and is reasonable. Of the total charges transferred to the zinc ion, most come from Asp295 (Oδ2 atom), and a very small amount of charges are transferred from the histidine residues (Table 1). The total charge of Asp295 is significantly reduced, from −1.0 to −0.4. Charge distribution within a residue also differs from that of AMBER. In the histidine residues, the negative charges of Nε atoms decrease, due to charge transfer to the zinc ion, while the electron populations increase on the adjacent Cε and Cδ atoms. These charge distributions might be important to reproduce reasonable coordination geometry around the zinc ion during MD simulations.

The coordination bond parameters are listed in Table 2. The force constants proposed here are much smaller than those of usual covalent bonds in AMBER; the force constants of usual covalent bonds are on the order of several hundreds (kcal/mol/Å^2). Our force constants, 18−35 kcal/mol/Å^2, are rather small compared with those of the bonded approach introduced by Merz et al.,[32−36] which are 40−100 kcal/mol/Å^2. In our model, the weaker bonds are compensated by nonbonded interactions. This is the most characteristic point of our model. The next section demonstrates that our coordination bond model well reproduces experimental coordination bond structures.

Structures and Interaction Energies. First, we discuss the active site geometry of ADA-inhibitor complexes obtained from MD simulations. The average geometric parameters are shown in Tables 3 and 4, along with experimental values. Average coordination bond distances agreed well with experiments within an error of 0.3 Å, except for zinc-water in complex **4** (Table 3). The average angles are also in good agreement with experimental values (Table 4); almost all angles are within the minimum and maximum values observed in crystal structures. Thus, using the new coordination bond parameters, the experimental geometry of residues around the zinc ion, five-atom coordination, is satisfactorily reproduced by the MD simulations. Moreover, the standard deviation of coordination bond angles indicates that the coordination bonds are sufficiently flexible (Table 4).

MD simulations on the same ADA-inhibitor complexes with standard AMBER parameters resulted in four- or six-atom coordination structures. Our coordination bond model reproduced the proper coordination number and the distances and angles of the coordination bonds. Hence, our model is applicable to binding free energy calculations, for which rather long simulations are required.

Next, we examine the accuracy of the average interaction energies between inhibitor molecules and their environment. The standard deviations and errors of the interaction energies are evaluated from the average values from snapshots taken every 50 ps, in 500 ps trajectories (Table 5). The maximum standard deviation is 5.3 kcal/mol, suggesting that system fluctuation is rather large, especially in the bound state, while the standard errors are very small for both bound and unbound states. Therefore, it can be said that equilibration and sampling runs were performed adequately for calculating binding free energy using eq 1.

Finally, we briefly mention the effect of solvent molecules on the conformations of the solute molecules. Since the inhibitor molecules are almost buried in the protein binding pocket, the significant effect was observed only in the unbound state. There are two amide groups in the inhibitors **5**, **6**, and **7**, and the groups are facing each other in the bound state, as shown in Figure 3(a). On the contrary, a water-

Table 4. Average Coordination Bond Angles (degrees)[a]

angle	2	3	4	7	min[b]	max[c]
15Nϵ-Zn-17Nϵ	108.9(9.8)	104.8(9.9)	103.1(9.8)	111.6(8.8)	111.2	121.8
15Nϵ-Zn-214Nϵ	88.3(4.2)	89.0(4.9)	87.3(4.8)	88.4(4.5)	83.0	96.1
15Nϵ-Zn-295Oδ	88.3(5.2)	87.3(5.1)	87.6(5.4)	88.8(5.3)	85.1	97.2
15Nϵ-Zn-WAT	106.4(11.0)	105.1(12.4)	101.3(10.5)	108.7(11.3)	104.3	113.9
17Nϵ-Zn-214Nϵ	90.5(4.9)	92.7(5.0)	89.7(4.8)	92.9(4.8)	88.9	93.7
17Nϵ-Zn-295Oδ	95.6(5.8)	91.9(5.8)	92.2(5.3)	90.7(5.2)	87.8	103.3
17Nϵ-Zn-WAT	143.8(12.5)	147.3(15.5)	153.4(13.9)	138.6(12.7)	131.6	138.6
214Nϵ-Zn-295Oδ	170.8(4.5)	171.0(4.5)	171.5(4.4)	172.3(4.4)	162.8	176.5
214Nϵ-Zn-WAT	93.3(5.3)	94.5(5.3)	95.3(5.3)	93.3(5.1)	94.8	105.7
295Oδ-Zn-WAT	82.6(4.4)	82.5(4.5)	84.4(5.0)	85.2(5.5)	68.4	80.3

[a] Standard deviation are in parentheses. [b] Minimum values observed in crystal structures (1NDW, 1NDY, modified 2E1W, and 1NDZ). [c] Maximum values observed in the crystal structures.

Table 5. Standard Deviations and Standard Errors of Interaction Energies (kcal/mol)[a]

	standard deviation				standard error			
inhibitor	V_w^{vdw}	V_w^{ele}	V_p^{vdw}	V_p^{ele}	V_w^{vdw}	V_w^{ele}	V_p^{vdw}	V_p^{ele}
1	0.3	1.5	0.6	1.9	0.1	0.5	0.2	0.6
2	1.5	1.8	1.5	3.2	0.5	0.6	0.5	1.0
3	0.3	1.2	1.1	3.4	0.1	0.4	0.4	1.1
4	0.3	1.7	0.9	1.5	0.1	0.5	0.3	0.5
5	0.8	1.5	1.8	1.5	0.2	0.5	0.6	0.5
6	0.2	3.0	0.7	2.1	0.1	1.0	0.2	0.7
7	0.7	5.3	0.8	1.0	0.2	1.7	0.3	0.3

[a] V^{vdw} and V^{ele} are van der Waals and electrostatic interaction energies, respectively. The subscripts w and p indicate the unbound and bound states of the inhibitors, respectively.

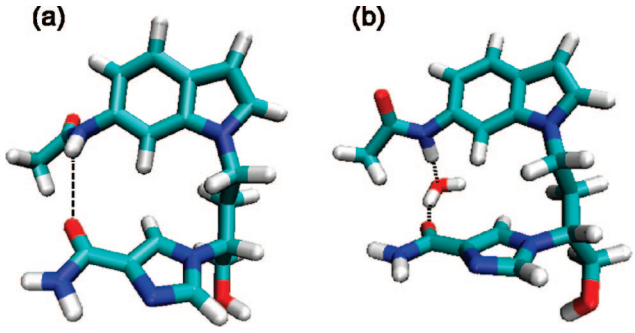

Figure 3. The conformations of inhibitor **5** observed in the bound state simulation (a) and in the unbound state simulation (b). In the conformation (a), two amide groups in the molecule face each other, and in the conformation (b), one water molecule intermediates the two amide moieties by hydrogen bonds. Hydrogen bonds are depicted with dashed lines.

mediated conformation (Figure 3(b)) is often observed in the unbound state. Such a conformation has the larger solute−solvent interaction energy than that in the bound state. The large standard deviations of the interaction energies for the inhibitors in the unbound states might be a reflection of the fact (Table 5).

Binding Free Energies. The binding free energies of seven ADA inhibitors, calculated by the LIE method, are summarized in Table 6. In these calculations the coefficients β and α are taken as 0.5 and 0.28, respectively (eq 1); the former was derived from the linear response approximation, and the latter came from fitting calculated binding free energies to experimental ones. Wang et al. reported that the parameter α describes a ratio factor of the van der Waals interaction and the nonpolar desolvation energy and depends on the nature of protein active site.[24] The value of 0.28 obtained in this study is within the range of the reported values for various proteins, 0.14−1.043.[18−20,22−24,26,28]

The calculated binding free energies successfully reproduce the experimental values. The mean unsigned error is 0.8 kcal/mol, and the correlation coefficient is 0.90. The results indicate a tendency of overestimation of ΔG_{bind} for low affinity inhibitors, especially inhibitors **1** and **2**. This might be partially because these affinities are measured for racemates, and active isomers are expected to have higher affinities. Though we did not evaluate the predictive ability of the model using test set compounds, the leave-one-out analysis, a method to evaluate the prediction power of a model, showed the high cross-validated q^2 value of 0.70. Hence, our model is expected to give a good prediction for a new compound with a similar framework, because the compounds with various molecular sizes and wide range activities evenly distributed were selected as the training set. However, it should be noted that a high q^2 value does not always lead to the high external predictive ability of a model.[49]

The van der Waals interactions of inhibitors in both bound and unbound states, $<V_p^{vdw}>$ and $<V_w^{vdw}>$, are increased as molecular size increases. This tendency is reasonable, as Åqvist et al. showed that mean nonpolar interaction energies depend linearly on molecular size.[18] The differences between the van der Waals interaction energies of bound and unbound states, $\Delta V_{p-w}^{vdW} = \langle V_p^{vdW} \rangle - \langle V_w^{vdW} \rangle$, are also larger for larger molecules. Thus, a larger molecule is preferable for binding as long as there is sufficient space at the protein binding site.

On the other hand, the difference between the electrostatic interaction energies of bound and unbound states does not simply correlate with molecular size, but is a delicate balance between the two states. For instance, the electrostatic term ΔV_{p-w}^{ele} of inhibitor **7** is not much larger than that of the others, despite its electrostatic interaction with the environment being significantly larger. The large electrostatic energy in the bound state is mostly canceled by the comparable electrostatic energy in the unbound state, which is called the desolvation penalty. Thus, the net electrostatic contribution of inhibitor **7** is not significantly larger than that of the others.

Methyl Substitution Effects. Inhibitor **4** is a methylated derivative of inhibitor **3** (Figure 2). By introducing a methyl group, the binding affinity is improved about 60 times. It is believed that the affinity increase is achieved by additional

Table 6. Calculated Binding Free Energies and Their Components (in kcal/mol)

inhibitor	$<V_w^{vdw}>$	$<V_w^{ele}>$	$<V_p^{vdw}>$	$<V_p^{ele}>$	$\Delta V_{p\text{-}w}^{vdw}$ [a]	$\Delta V_{p\text{-}w}^{ele}$ [b]	ΔG_{bind} (calc)	ΔG_{bind} [c] (exp)	error[d]
1	−16.7	−52.6	−28.8	−59.2	−12.1	−6.5	−6.7	−5.9	0.8
2	−21.1	−54.4	−37.0	−61.4	−15.9	−6.9	−7.9	−7.2	0.8
3	−24.0	−55.6	−39.7	−63.0	−15.7	−7.4	−8.1	−8.5	0.4
4	−25.1	−56.2	−43.3	−65.5	−18.2	−9.3	−9.7	−10.9	1.2
5	−25.9	−66.6	−46.1	−73.0	−20.2	−6.4	−8.9	−8.1	0.8
6	−32.0	−65.6	−56.4	−70.5	−24.4	−4.8	−9.3	−10.5	1.2
7	−35.5	−81.2	−65.2	−87.9	−29.7	−6.7	−11.7	−11.1	0.5

[a] Difference in van der Waals interaction energies between bound and unbound states; $\Delta V_{p-w}^{vdw} = <V_p^{vdw}> - <V_w^{vdw}>$. [b] Difference in electrostatic interaction energies between bound and unbound states; $\Delta V_{p-w}^{ele} = <V_p^{ele}> - <V_w^{ele}>$. [c] Inhibition constants K_i[14−17] are regarded as dissociation constants K_d and converted to ΔG_{bind}. [d] $|\Delta G_{bind}(calc) - \Delta G_{bind}(exp)|$.

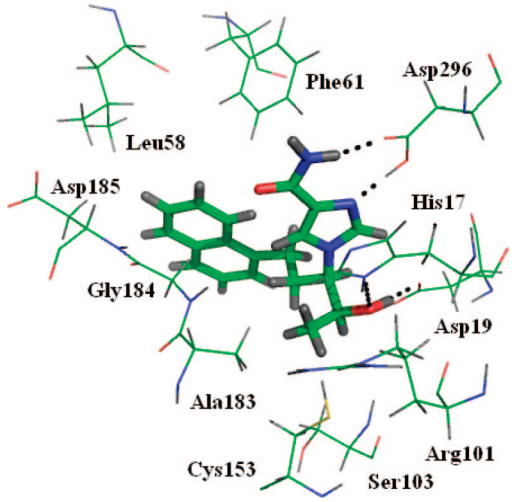

Figure 4. Amino acid residues around inhibitor **4**. The inhibitor molecule is shown with the thick line. Hydrogen bonds are depicted with dashed lines.

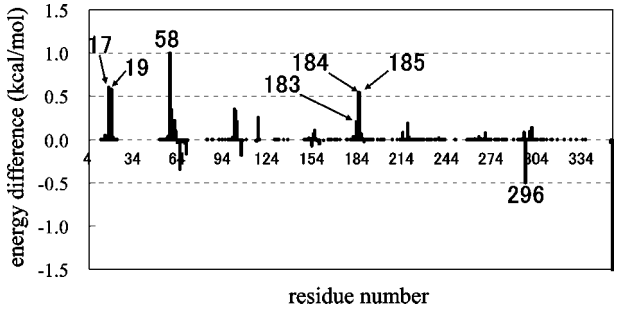

Figure 5. Difference in the average van der Waals interaction energy between inhibitors **3** and **4**, [**3**−**4**]. Residue numbers 353 and 354 are zinc ions and water molecules, respectively.

van der Waals interactions of the methyl group with neighboring residues: His17, Ser103, Cys153, and Ala183 (Figure 4).

To clarify this phenomenon, the average interaction energy is decomposed into individual contributions from each residue-inhibitor interaction. Figure 5 shows the difference in van der Waals interaction energy between inhibitor **3** and **4**. Ala183, which is the closest residue to the methyl group, does not have a large difference, while Gly184 and Asp185 have large differences. Moreover, large differences are observed in the residues His17, Asp19, Leu58, and Asp296. These residues, except His17, are not close to the methyl group but are located around the inhibitor molecules. This suggests that the average positions in the binding pocket differ slightly between the two inhibitors.

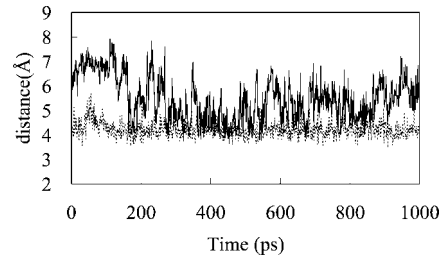

Figure 6. Distance between Gly184(Cα) and naphthyl(C4a) of the inhibitor during a 1 ns run after equilibration: inhibitor **3** (solid line) and inhibitor **4** (dashed line).

The largest difference in average distances is found between the C4a atom (inhibitor) and the Cα atom (Gly184); 5.47 and 4.22 Å for inhibitors **3** and **4**, respectively. The fluctuation of the distance during MD simulations is considerably different, as shown in Figure 6; the fluctuation in inhibitor **3** is apparently larger than that in inhibitor **4**. The standard deviations are 0.9 and 0.3 Å for inhibitors **3** and **4**, respectively. Gly184 is adjacent to Ala183 and does not contact the methyl group introduced into the inhibitor, but its mobility is significantly affected. This can be understood as follows. Ala183, whose side chain methyl group is in contact with the methyl group and covalently linked adjacent Gly184 are restrained to a certain extent from moving together. This produces a shorter average distance and larger van der Waals interactions with Gly184 in the inhibitor **4** complex. Such differences in dynamic fluctuation should be taken into consideration when predicting affinity change by methyl substitution in an inhibitor molecule. Note that the difference between the distance fluctuations in inhibitors **3** and **4** is consistent with the standard deviation of interaction energy (Table 5); the standard deviation of electrostatic interaction energy in the protein is larger for inhibitor **3** than for **4**.

CONCLUSION

Novel coordination bond parameters for zinc ions were generated and applied to MD simulations of ADA-inhibitor complexes. The binding free energies calculated with the LIE method were in good agreement with experiments, where the average interaction energies obtained from the MD simulations were used. Moreover, we succeeded in reproducing the experimentally observed affinity improvement by introducing a methyl group into the inhibitors. Analyzing the MD trajectories, we found that the affinity improvement was realized by the combination of additional van der Waals interactions of the introduced methyl group with contact

residues and tightened overall interactions of the molecule by changing the average position in the binding pocket. For predicting the affinity change, we suggest that the change in dynamic fluctuation of inhibitors in the protein binding pocket should be taken into consideration. The results presented in this work are expected to be useful in structure-based drug design.

ACKNOWLEDGMENT

This work is partially supported by a Grant-in-Aid for Scientific Research (C18590096), JSPS. I.N. and K.K. thank Astellas Pharma Inc. for financial support.

Supporting Information Available: All atomic partial charges used in MD simulations. This material is available free of charge via the Internet at http://pubs.acs.org.

REFERENCES AND NOTES

(1) Harms, A. F.; Nauta, W. Th. The effects of alkyl substitution in drugs. I. substituted dimethylaminoethyl benzhydryl ethers. *J. Med. Pharm. Chem.* **1960**, *2*, 57–77.
(2) Black, E.; Breed, J.; Breeze, A. L.; Embrey, K.; Garcia, R.; Gero, T. W.; Godfrey, L.; Kenny, P. W.; Morley, A. D.; Minshull, C. A.; Pannifer, A. D.; Read, J.; Rees, A.; Russell, D. J.; Toader, D.; Tucker, J. Structure-based design of protein tyrosine phosphatase-1B inhibitors. *Bioorg. Med. Chem. Lett.* **2005**, *15*, 2503–2507.
(3) Lambrinidis, G.; Halabalaki, M.; Katsanou, E. S.; Skaltsounis, A.; Alexis, M. N.; Mikros, E. The estrogen receptor and polyphenols: molecular simulation studies of their interactions, a review. *Environ. Chem. Lett.* **2006**, *4*, 159–174.
(4) Thompson, L. F.; Seegmiller, J. E. Adenosine deaminase deficiency and severe combined immunodeficiency disease. *Adv. Enzymol.* **1980**, *51*, 167–210.
(5) Valenzuela, A.; Blanco, J.; Callebaut, C.; Jacotot, E.; Lluis, C.; Hovanessian, A. G.; Franco, R. Adenosine deaminase binding to human CD26 is inhibited by HIV-1 envelope glycoprotein gp120 and viral particles. *J. Immunol.* **1997**, *158*, 3721–3729.
(6) Simpkins, H.; Stanton, A.; Davis, B. H. Adenosine deaminase activity in lymphoid subpopulations and leukemias. *Cancer Res.* **1981**, *41*, 3107–3110.
(7) Nakamachi, Y.; Koshiba, M.; Nakazawa, T.; Hatachi, S.; Saura, R.; Kurosaka, M.; Kusaka, H.; Kumagai, S. specific increase in enzymatic activity of adenosine deaminase 1 in rheumatoid synovial fibroblasts. *Arthritis Rheum.* **2003**, *48*, 668–674.
(8) Yuksel, H.; Akoglu, T. F. Serum and synovial fluid adenosine deaminase activity in patients with rheumatoid arthritis, osteoarthritis, and reactive arthritis. *Ann. Rheum. Dis.* **1988**, *47*, 492–495.
(9) Ralevic, V.; Burnstock, G. Receptors for purines and pyrimidines. *Pharmacol. Rev.* **1998**, *50*, 536–543.
(10) Olsson, R. A.; Pearson, J. D. Cardiovascular purinoceptors. *Physiol. Rev.* **1990**, *70*, 413–492.
(11) Shryock, J. C.; Belardinelli, L. Adenosine and adenosine receptors in the cardiovascular system: Biochemistry, physiology, and pharmacology. *Am. J. Cardiol.* **1997**, *79*, 2–10.
(12) Guieu, R.; Dussol, B.; Halimi, G.; Bechis, G.; Sampieri, F.; Berland, Y.; Sampol, J.; Courand, F.; Rochat, H. Adenosine and the nervous system: Pharmacological data and therapeutic perspectives. *Gen. Pharmacol.* **1998**, *31*, 553–561.
(13) Ohta, A.; Sitkovsky, M. Role of G-protein-coupled adenosine receptors in downregulation of inflammation and protection from tissue damage. *Nature* **2001**, *414*, 916–920.
(14) Terasaka, T.; Nakanishi, I.; Nakamura, K.; Eikyu, Y.; Kinoshita, T.; Nishio, N.; Sato, A.; Kuno, M.; Seki, N.; Sakane, K. Structure-based De novo design of non-nucleoside adenosine deaminase inhibitors. *Bioorg. Med. Chem. Lett.* **2003**, *13*, 1115–1118.
(15) Terasaka, T.; Kinoshita, T.; Kuno, M.; Nakanishi, I. A highly potent non-nucleoside adenosine deaminase inhibitor: Efficient drug discovery by intentional lead hybridization. *J. Am. Chem. Soc.* **2004**, *126*, 34–35.
(16) Terasaka, T.; Okumura, H.; Tsuji, K.; Kato, T.; Nakanishi, I.; Kinoshita, T.; Kato, Y.; Kuno, M.; Seki, N.; Naoe, Y.; Inoue, T.; Tanaka, K.; Nakamura, K. Structure-based design and synthesis of non-nucleoside, potent, and orally bioavailable adenosine deaminase inhibitors. *J. Med. Chem.* **2004**, *47*, 2728–2731.
(17) Terasaka, T.; Kinoshita, T.; Kuno, M.; Seki, N.; Tanaka, K.; Nakanishi, I. Structure-based design, synthesis, and structure-activity relationship studies of novel non-nucleoside adenosine deaminase Inhibitors. *J. Med. Chem.* **2004**, *47*, 3730–3743.
(18) Åqvist, J.; Medina, C.; Samuelsson, J. E. A new method for predicting binding affinity in computer-aided drug design. *Protein Eng.* **1994**, *7*, 385–391.
(19) Hansson, T.; Åqvist, J. Estimation of binding free energies for HIV proteinase inhibitors by molecular dynamics simulations. *Protein Eng.* **1995**, *8*, 1137–1144.
(20) Hultén, J.; Bonham, N. M.; Nillroth, U.; Hansson, T.; Zuccarello, G.; Bouzide, A.; Åqvist, J.; Classon, B.; Danielson, U. H.; Karlén, A.; Kvarnström, I.; Samuelsson, B.; Hallberg, A. Cyclic HIV-1 protease inhibitors derived from mannitol: synthesis, inhibitory potencies, and computational predictions of binding affinities. *J. Med. Chem.* **1997**, *40*, 885–897.
(21) Zoete, V.; Michielin, O.; Karplus, M. Protein-ligand binding free energy estimation using molecular mechanics and continuum electrostatics. Application to HIV-1 protease inhibitors. *J. Comput.-Aided Mol. Des.* **2003**, *17*, 861–880.
(22) Åqvist, J.; Mowbray, L. S. Sugar recognition by a glucose/galactose receptor. *J. Biol. Chem.* **1995**, *270*, 9978–9981.
(23) Marelius, J.; Hansson, T.; Åqvist, J. Calculation of ligand binding free energies from molecular dynamics simulations. *Int. J. Quantum Chem.* **1998**, *69*, 77–88.
(24) Wang, W.; Wang, J.; Kollman, P. A. What determines the van der Waals coefficient β in the LIE (linear interaction energy) method to estimate binding free energies using molecular dynamics simulations. *Proteins* **1999**, *34*, 395–402.
(25) Jones-Hertzog, D. K.; Jorgensen, W. L. Binding affinities for sulfonamide inhibitors with human thrombin using monte carlo simulations with a linear response method. *J. Med. Chem.* **1997**, *40*, 1539–1549.
(26) Lamb, M. L.; Tirado-Rives, J.; Jorgensen, W. L. Estimation of the binding affinities of FKBP12 inhibitors using a linear response method. *Bioorg. Med. Chem.* **1999**, *7*, 851–860.
(27) Zhou, R.; Friesner, R. A.; Ghosh, A.; Rizzo, R. C.; Jorgensen, W. L.; Levy, R. M. New linear interaction method for binding affinity calculations using a continuum solvent model. *J. Phys. Chem. B* **2001**, *105*, 10388–10397.
(28) Paulsen, M. D.; Ornstein, R. L. Binding free energy calculations for P450cam-substrate complexes. *Protein Eng.* **1996**, *9*, 567–571.
(29) Smith, R. H.; Jorgensen, W. L.; Tirado-Rives, J.; Lamb, M. L.; Jenssen, P. A. J.; Michejda, C. J.; Smith, M. B. K. Prediction of binding affinities for TIBO inhibitors of HIV-1 reverse transcriptase using monte carlo simulations in a linear response method. *J. Med. Chem.* **1998**, *41*, 5272–5286.
(30) Hou, T.; Guo, S.; Xu, X. Predictions of binding of a diverse set of ligands to gelatinase-A by a combination of molecular dynamics and continuum solvent models. *J. Phys. Chem. B* **2002**, *106*, 5527–5535.
(31) Merz, K. M., Jr. CO_2 binding to human carbonic anhydrase II. *J. Am. Chem. Soc.* **1991**, *113*, 406–411.
(32) Hoops, S. C.; Anderson, K. W.; Merz, K. M., Jr. Force field design for metalloproteins. *J. Am. Chem. Soc.* **1991**, *113*, 8262–8270.
(33) Toba, S.; Colombo, G.; Merz, K. M., Jr. Solvent dynamics and mechanism of proton transfer in human carbonic anhydrase II. *J. Am. Chem. Soc.* **1999**, *121*, 2290–2302.
(34) Suarez, D.; Merz, K. M., Jr. Molecular dynamics simulations of the mononuclear zinc-β-lactamase from Bacillus Cereus. *J. Am. Chem. Soc.* **2001**, *123*, 3759–3770.
(35) Suarez, D.; Brothers, E. N.; Merz, K. M., Jr. Insights into the structure and dynamics of the dinuclear zinc β-lactamase site from Bacteroides fragilis. *Biochemistry* **2002**, *41*, 6615–6630.
(36) Suarez, D.; Diaz, N.; Merz, K. M., Jr. Molecular dynamics simulations of the dinuclear zinc-β-lactamase from *Bacteroides fragilis* Complexed with Imipenem. *J. Comput. Chem.* **2002**, *23*, 1587–1600.
(37) Vedani, A.; Huhta, D. W. A new force field for modeling metalloproteins. *J. Am. Chem. Soc.* **1990**, *112*, 4759–4767.
(38) Stone, R. H.; Karplus, M. Zinc Binding in Proteins and Solution: A simple but accurate nonbonded representation. *Proteins: Struct., Funct., Genet.* **1995**, *23*, 12–31.
(39) Alberts, I. L.; Nadassy, K.; Wodak, S. J. Analysis of zinc binding sites in protein crystal structures. *Protein Sci.* **1998**, *7*, 1700–1716.
(40) Besler, B. H.; Merz, K. M., Jr.; Kollman, P. A. Atomic charges derived from semiempirical methods. *J. Comput. Chem.* **1990**, *11*, 431–439.
(41) Wilson, D. K.; Quiocho, F. A. A pre-transition-state mimic of an enzyme: X-ray structure of adenosine deaminase with bound 1-deazaadenosine and zinc-activated water. *Biochemistry* **1993**, *32*, 1689–1694.
(42) Case, D. A.; Darden, T. A.; Cheatham, T. E., III; Simmerling, C. L.; Wang, J.; Duke, R. E.; Luo, R.; Merz, K. M.; Wang, B.; Pearlman, D. A.; Crowley, M.; Brozell, S.; Tsui, V.; Gohlke, H. ; Mongan, J.; Hornak, V.; Cui, G.; Beroza, P.; Schafmeister, C.; Caldwell, J. W.;

Ross, W. S.; Kollman, P. A. *AMBER 8*; University of California, San Francisco: San Francisco, CA, 2004.

(43) Frisch, M. J.; Trucks, G. W.; Schlegel, H. B.; Scuseria, G. E.; Robb, M. A.; Cheeseman, J. R.; Montgomery, J. A., Jr.; Vreven, T.; Kudin, K. N.; Burant, J. C.; Millam, J. M. ; Iyengar, S. S.; Tomasi, J.; Barone, V.; Mennucci, B.; Cossi, M.; Scalmani, G.; Rega, N.; Petersson, G. A.; Nakatsuji, H.; Hada, M.; Ehara, M.; Toyota, K.; Fukuda, R.; Hasegawa, J.; Ishida, M.; Nakajima, T.; Honda, Y.; Kitao, O.; Nakai, H.; Klene, M.; Li, X.; Knox, J. E.; Hratchian, H. P.; Cross, J. B.; Adamo, C.; Jaramillo, J.; Gomperts, R.; Stratmann, R. E.; Yazyev, O.; Austin, A. J.; Cammi, R.; Pomelli, C.; Ochterski, J. W.; Ayala, P.; Morokuma, Y. K.; Voth, G. A.; Salvador, P.; Dannenberg, J. J.; Zakrzewski, V. G.; Dapprich, S.; Daniels, A. D.; Strain, M. C.; Farkas, O.; Malick, D. K.; Rabuck, A. D.; Raghavachari, K.; Foresman, J. B.; Ortiz, J. V.; Cui, Q.; Baboul, A. G.; Clifford, S.; Cioslowski, J.; Stefanov, B. B.; Liu, G.; Liashenko, A.; Piskorz, P.; Komaromi, I.; Martin, R. L.; Fox, D. J.; Keith, T.; Al-Laham, M. A. Peng, C. Y.; Nanayakkara, A.; Challacombe, M.; Gill, P. M. W.; Johnson, B.; Chen, W.; Wong, M. W.; Gonzalez, C.; Pople, J. A. *Gaussian 03, Revision C.02*; Gaussian, Inc.: Wallingford, CT, 2004.

(44) Wang, J.; Cieplak, P.; Kollman, P. A. How well does a restrained electrostatic potential (RESP) model perform in calculating conformational energies of organic and biological molecules. *J. Comput. Chem.* **2000**, *21*, 1049–1074.

(45) Bayly, C. I.; Cieplak, P.; Cornell, W. D.; Kollman, P. A. A well-behaved electrostatic potential based method using charge restraints for deriving atomic charges: The RESP model. *J. Phys. Chem.* **1993**, *97*, 10269–10280.

(46) Wang, J.; Wolf, R. M.; Caldwell, J. W.; Kollman, P. A.; Case, D. A. Development and testing of a general AMBER force field. *J. Comput. Chem.* **2004**, *25*, 1157–1174.

(47) Jorgensen, W. L.; Chandrasekhar, J.; Madura, J. D.; Impey, R. W.; Klein, M. L. Comparison of simple potential functions for simulating liquid water. *J. Chem. Phys.* **1983**, *79*, 926–935.

(48) Essman, V.; Perera, L.; Berkowitz, M. L.; Darden, T.; Lee, H.; Pedersen, L. G. A Smooth particle-mesh-ewald method. *J. Chem. Phys.* **1995**, *103*, 8577–8593.

(49) Golbraikh, A.; Tropsha, A. Beware of q2! *J. Mol. Graphics Modell.* **2002**, *20*, 269–276.

CI8002667